Final Report

Project Title: Investigation of changes in conformation and oligomeric state of the nucleotide excision repair proteins during repair reaction

By

Danaya Pakotiprapha, Ph.D.

May 2016

Contract No. MRG5680043

Final Report

Project Title: Investigation of changes in conformation and oligomeric state of the nucleotide excision repair proteins during repair reaction

By

Danaya Pakotiprapha, Ph.D.
Mahidol University

This project granted by the Thailand Research Fund

1. Abstract

Project Code : MRG5680043

Project Title : Investigation of changes in conformation and oligomeric state of the nucleotide excision repair proteins during repair reaction

Investigator : Danaya Pakotiprapha, Ph.D.

E-mail Address : danaya.pak@mahidol.ac.th

Project Period : 3 June 2013 – 2 June 2015

Abstract:

Nucleotide excision repair (NER) is distinguished from other DNA repair pathways by its ability to correct a wide range of structurally and chemically unrelated DNA lesions. UvrA is the key bacterial NER protein that recognizes DNA damage. Together with UvrB, it forms $UvrA_2B_2$ complex that searches for the lesion and triggers a downstream repair cascade that restores the DNA. Unlike other NER proteins, UvrA can bind to DNA without other NER components. Based on previous structural and biochemical data, models have been proposed for how UvrA discriminates damaged from undamaged DNA through interconversion between the 'open dimer' and 'closed dimer' conformations, and for how two UvrB molecules could function to select the appropriate DNA strand for incision.

We proposed to use a combination of biochemical and biophysical methods to test the described models. Although we were not able to dissect the roles of the transition between 'open dimer' and 'closed dimer' conformations of UvrA, our results showed, for the first time, that the conformational change of the β-hairpin of the third Zn module of UvrA (Zn3hp) is crucial for lesion recognition. The movement of Zn3hp is controlled by ATP hydrolysis at the distal nucleotide binding site, and is required for damage-sensing, ATP hydrolysis and UvrB loading.

Keywords : nucleotide excision repair, DNA repair, UvrA, disulfide crosslinking

Table of Contents

1. Abstract ii

Table of contents iii

List of figures iv

2. Executive summary 1

3. Objectives 3

4. Research methodology 4

5. Results

5.1 Expression and purification of UvrA cysteine mutants 9

5.2 All UvrA cysteine mutants have intact ATPase and DNA binding activities 9

5.3 Crosslinking studies of UvrA in the 'open dimer' and 'closed dimer' conformation 13

5.4 Trapping of the β-hairpin of the third zinc-binding module (Zn3hp) in the 'closed' conformation 16

5.5 Conformational change of Zn3hp is crucial for damage-specific DNA binding 18

5.6 Movement of Zn3hp is required for UvrB loading 20

5.7 Movement of Zn3hp is essential for ATP hydrolysis 21

5.8 ATP hydrolysis at the distal nucleotide binding site mediates the movements of Zn3hp 22

5.9 Characterization of the UvrB 'dimer' 25

6. Conclusion and discussion

6.1 UvrA uses different DNA binding modes to interact with DNA 26

6.2 ATP hydrolysis at the distal site increases the dynamics of the Zn3hp 28

6.3. Conclusion 28

7. Output 29

8. References 30

List of Figures

Figure 1	'Open dimer' and 'closed dimer' conformations of UvrA	4
Figure 2	Locations of designed disulfide pairs for UvrA in the 'open dimer' and 'closed dimer' conformations	5
Figure 3	The UvrB 'dimer'	8
Figure 4	Purification of UvrA cysteine mutants	9
Figure 5	UvrA cysteine mutants have intact ATPase activity	10
Figure 6	UvrA cysteine mutants have intact DNA-binding activity	11
Figure 7	Crosslinking of UvrA in the 'open dimer' conformation	14
Figure 8	Crosslinking of UvrA in the 'closed dimer' conformation	15
Figure 9	Conformational change of signature domain II and Zn3hp upon DNA binding	17
Figure 10	The movement of Zn3hp is required for damage-specific binding	19
Figure 11	The limited movement of Zn3hp disrupts UvrB loading activity	20
Figure 12	The movement of Zn3hp is required for ATP hydrolysis	21
Figure 13	ATP binding/ ATP hydrolysis at distal site controls the conformational change between open and closed β-hairpin	23
Figure 14	ATP hydrolysis by ATPase wild-type and mutant UvrA	24
Figure 15	DNA binding properties of UvrB 'momoner' and 'dimer' fractions	25
Figure 16	Model for lesion recognition by UvrA	26

2. EXECUTIVE SUMMARY

2.1 Background and significance

Nucleotide excision repair (NER) is distinguished from other DNA repair pathways by its ability to recognize and repair structurally and chemically unrelated DNA lesions. In bacteria, UvrA and UvrB are responsible for the initial steps of NER. Together they form $UvrA_2B_2$ complex that searches for the lesion and triggers a downstream repair cascade that restores the DNA. Unlike other NER proteins, UvrA can bind to DNA without other NER components. Based on previous structural and biochemical data, a model has been proposed for how UvrA discriminates damaged from undamaged DNA through interconversion between the 'open dimer' and 'closed dimer' conformations. In addition, it has also been suggested that each of the two UvrB molecules functions to probe each DNA strand for the presence of damage, and upon localization to the lesion, determine which strand needs to be cleaved.

We proposed to use a combination of biochemical and biophysical methods to study the conformational change of UvrA dimer, how such changes are regulated by nucleotides, and how they might be used in lesion detection. We also proposed to characterize biochemical properties of the purified UvrB dimer to better understand its role in damage recognition and strand selection.

Understanding the mechanism of DNA damage recognition is important as DNA repair is a fundamental process that is found in all organisms, and it is crucial for the maintenance of genetic information. Insights into lesion recognition in bacterial NER will also provide a basis for understanding human NER, which, although carried out by unrelated proteins, utilizes the same overall mechanism.

2.2 Objectives

2.2.1 To study the role of conformational changes of UvrA in DNA damage recognition and how such changes are regulated by nucleotide

2.2.2 To study the properties of UvrB dimer, and whether the UvrB dimer plays a role in selection of the damaged DNA strand for repair

2.3 Results and discussion

Site-specific disulfide crosslinking was used to probe how different factors, including nucleotide, UvrB, damaged and undamaged DNA, affect the interconversion between the 'open dimer' and 'closed dimer' conformations of UvrA. Due to low crosslinking efficiencies observed for the disulfide pairs designed based on the 'closed

dimer' conformation, we were not able to dissect the roles of the conformational change in UvrA dimer in damage detection. We observed, however, that crosslinking at the H750C-H750C site is dramatically influenced by the presence of DNA and ATP, suggesting that β-hairpin of the third Zn module of UvrA (Zn3hp), on which H750 is located, could play a crucial role in lesion recognition. We proceeded to show, for the first time, that the conformational change of Zn3hp is crucial for lesion recognition. The movement of Zn3hp is controlled by ATP hydrolysis at the distal nucleotide binding site, and is required for damage-sensing, ATP hydrolysis and UvrB loading.

Analysis of UvrB using analytical centrifugation and fluorescence spectroscopy suggested that what was previously thought of as the UvrB 'dimer' fraction is likely UvrB monomer in complex with a sub-stoichiometric contaminant. Attempts to identify this contaminant by mass spectrometry have so far been unsuccessful.

2.4 Output

2.4.1 One munuscript is being prepared for submission to the journals *Nucleic Acid Research*, *DNA Repair*, or *Mutation Research.*

Kraithong T*., Channgam K*., Tiensuwan M., Itsathitphaisarn O., Jeruzalmi D., and Pakotiprapha D. *Movement of β-hairpin in the third zinc-binding module of UvrA is required for DNA damage detection.*

*These authors contributed equally to this work.

2.4.2 One proceeding has been published.

Channgam K. and Pakotiprapha D. *Expression, purification, and biochemical characterization of UvrA protein containing site-specific cysteine substitutions for monitoring of protein conformational change during DNA damage recognition.* The 10th International Symposium of The Protein Society of Thailand. 15-17 July 2015 Chulabhorn Research Institute.

3. OBJECTIVES

The overall goal of this work is to understand the mechanism of DNA damage recognition in bacterial nucleotide excision repair. We proposed to use biochemical, biophysical, and structural approaches to investigate the changes in conformation of UvrA and in oligomeric state of UvrB, and to determine how such changes are used in DNA damage recognition.

The specific objectives as included in the original proposal are as follow:

3.1 To study the role of conformational changes of UvrA in DNA damage recognition and how such changes are regulated by nucleotide

Previous structural studies of isolated UvrA and UvrA•UvrB complex showed that in addition to the 'open dimer' conformation that binds damaged DNA (Jaciuk et al., 2011), UvrA can also adopt a 'closed dimer' conformation, in which the DNA binding groove is likely only compatible with native, B-form DNA. We proposed that interconversion between 'open dimer' and 'closed dimer' conformations of UvrA could underlie the mechanism of discrimination between damaged and undamaged DNA. We planned to test this hypothesis by using conformation-specific disulfide bond formation as a tool to probe the conformational changes of UvrA in the absence or presence of different nucleotides, nucleotide analogs, UvrB, and/or damaged and undamaged DNA. The resulting crosslinked UvrA dimer would then be characterized using biochemical and structural techniques.

3.2 To study the properties of UvrB dimer, and whether the UvrB dimer plays a role in selection of the damaged DNA strand for repair

Our recent crystal structure of the $UvrA_2B_2$ complex suggests the involvement of two UvrB molecules in lesion recognition. Biochemical (Hildebrand and Grossman, 1999; Moolenaar et al., 2005) and structural (Webster et al., 2012) studies also suggest that UvrB might form dimer in solution. We proposed that UvrB dimer could play a role in lesion recognition by probing the two DNA strands for the presence of lesion and positioning the endonuclease UvrC for incision of the damaged strand. Working with *Geobacillus stearothermophilus* UvrB ortholog, we were able to separate stable UvrB dimer from UvrB monomer. We proposed to characterize the UvrB dimer by measuring its ATP binding, ATPase, and DNA binding activities, in comparison with those of the well-characterized UvrB monomer. In addition, we proposed to investigate the role of UvrB dimer-monomer transition in NER by subjecting a disulfide-trapped UvrB dimer to UvrC-mediated incision assay.

4. RESEARCH METHODOLOGY

4.1: Objective 1 To study the role of conformational changes of UvrA in DNA damage recognition and how such changes are regulated by nucleotide

In previous work, we have shown that the UvrA dimer could adopt two dramatically different conformations. In the 'open dimer' conformation, the DNA binding surface is wide and likely to bind both damaged and undamaged DNA, whereas in the 'closed dimer' conformation, the DNA binding site is transformed into a narrow groove that is likely compatible with only undamaged, B-form DNA (Figure 1). We proposed that interconversion of UvrA between the 'open dimer' and 'closed dimer' conformations could underlie the mechanism of DNA damage recognition (Pakotiprapha et al., 2012).

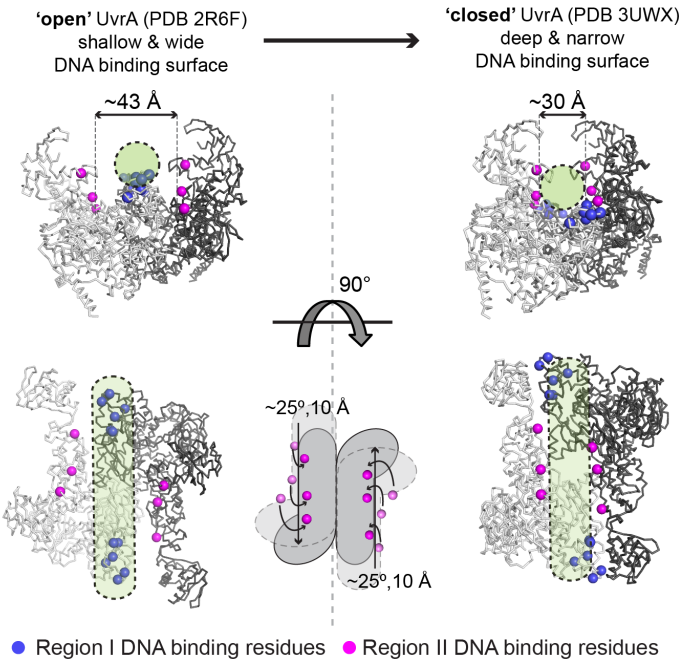

Figure 1 '**Open dimer' and 'closed dimer' conformations of UvrA.** Upon conformational change from 'open dimer' (left) to 'closed dimer' (right), the DNA binding groove is narrowed and additional residues (pink) come into contact with DNA (green cylinder).

In order to test this hypothesis and to elucidate how ATP binding and hydrolysis, and the presence of UvrB and/or DNA affect these conformational transition and lesion recognition, we proposed to use conformation-specific disulfide bond formation to probe UvrA conformational changes in response to different factors. Crystal structures of *Geobacillus stearothermophilus (Bst)* UvrA in the 'open dimer' (PDB 2R6F

(Pakotiprapha et al., 2008)) and 'closed dimer' (PDB 3UWX (Pakotiprapha et al., 2012)) conformations were analyzed by the program 'Disulfide by Design' (Craig and Dombkowski, 2013; Dombkowski, 2003). Disulfide by Design analyzes protein structure coordinates and identifies residue pairs that are likely to form disulfide bond if they are mutated to cysteines. These residue pairs are identified based on positions of backbone and C_β atoms that are consistent with the characteristics of known disulfides observed in previously determined protein structures.

Based on these analyses, we chose residue pairs that are predicted to form inter-chain disulfide bond specifically when the UvrA dimer is in the 'open dimer' or the 'closed dimer' conformation (Figure 2).

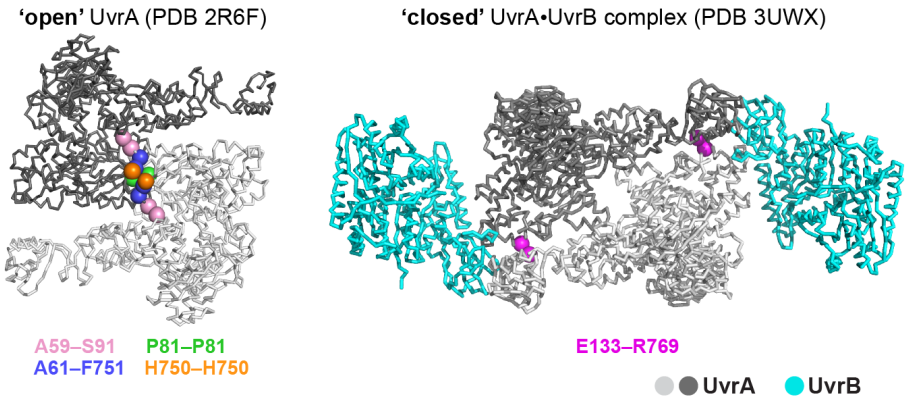

Figure 2 Locations of designed disulfide pairs for UvrA in the 'open dimer' and 'closed dimer' conformations.

Cysteine residues were individually substituted for the selected position by site-directed mutagenesis. The mutant proteins were expressed and purified using wild-type protocols and tested for ATPase, DNA binding, and UvrB loading activities to verify that the introduced cysteine mutation does not perturb protein function. All biochemical assays were carried out as described previously (Pakotiprapha et al., 2008) with the following modifications due to instrument limitations.

For ATPase assay, the rate of ATP hydrolysis was measured using a coupled enzyme system consisting of pyruvate kinase (Sigma-Aldrich) and lactate dehydrogenase (Sigma-Aldrich), where ATP hydrolysis is coupled with NADH oxidation. The 500-µl reaction contains 4 U lactate dehydrogenase, 2.5 U pyruvate kinase, 2 mM phosphoenolpyruvate (PEP), 250 µl/ml bovine albumin serum (BSA), 0.16 mM NADH in 50 mM K-HEPES pH 7.5, 150 mM potassium acetate, 8 mM magnesium acetate and 5

mM β-ME. The reaction mixture was incubated at 55°C for 5 minutes and the reaction was started by adding 1 mM ATP pH 7.0. Control reaction, without UvrA, was set up for background subtraction. The reaction was monitored for 30 minutes by measuring the decrease in A_{340}, which represents NADH oxidation coupled to ATP hydrolysis. Turnover number (k_{cat}), (mol ATP/min/mol UvrA) ± standard error (n=3) was reported. The effect of DNA on the rate of ATP hydrolysis was investigated by adding an equivalent of 10 μM bp of salmon sperm DNA into the assay.

For DNA binding assays, electrophoretic mobility shift assays (EMSAs) were visualized using SYBR-Gold fluorescent stain instead of ^{32}P-labelled DNA. Although the sensitivity of the fluorescent dye is lower than that of radioactive label, preliminary experiments with wild-type and known DNA binding mutants suggested that the new experimental conditions could recapitulate previous results. The assay was performed by titrating 20 nM five-nucleotide mismatched or undamaged DNA substrate with 0–200 nM UvrA in 50 mM Tris-HCl pH 7.5, 50 mM NaCl, 10 mM $MgCl_2$, 1 mM ATP, 5% (v/v) glycerol, 0.1 mg/ml BSA. The reactions were incubated at 55°C for 30 minutes, chilled on ice, then analyzed on 6% native polyacrylamide gel containing 10 mM $MgCl_2$ and 1 mM ATP in 0.5X Tris-borate. The gel was stained with SYBR-Gold (Invitrogen) and visualized by Typhoon scanner (GE Healthcare Life Sciences) using excitation wavelength of 488 nm and emission wavelength of 520 nm with 40 nm bandwidth.

UvrB loading was assayed in buffer consisting of 50 mM Tris-HCl pH 7.5, 100 mM NaCl, 10 mM $MgCl_2$ 1 mM ATP, 5% (v/v) glycerol, and 0.1 mg/ml BSA. This assay was performed by titrating 10 nM Alexa488-labeled DNA substrate and 5 nM UvrA with 0–200 nM UvrB. The reaction was incubated at 55°C for 10 minutes, chilled on ice, and analyzed on 6% native polyacrylamide gel containing 10 mM $MgCl_2$ and 1 mM ATP in 0.5X Tris-borate. The bands were visualized as described above.

Once it had been verified that the cysteine mutants were not functionally compromised, the proteins were incubated in non-reducing conditions to allow disulfide bond formation. β-ME was removed from UvrA by buffer exchange into 25 mM Tris-HCl pH 7.4, 400 mM NaCl using PD10 desalting column (GE Healthcare Life Sciences). Crosslinking reactions were set up using 1 μM of UvrA monomer in GF buffer 25 mM Tris-HCl pH 7.4, 400 mM NaCl containing different factors in damage recognition step. The factors in this assay include 1 μM Cys-less UvrB, 0.5 μM 50-mer DNA (undamaged or damaged), and 1 mM nucleotide in 10 mM $MgCl_2$. The reaction mixtures were incubated for 24 hours at room temperature. After 24-hour incubation, the reaction was stopped by adding non-reducing SDS-loading buffer with 20 mM *N*-ethylmaleimide. The samples were subsequently analyzed on 10% SDS-PAGE. Quantification of the band

intensities was carried out using ImageJ (Schneider et al., 2012) or ImageQuant software (GE Healthcare Life Sciences). The crosslinking efficiency was calculated as crosslink band intensity × 100 / total UvrA intensities. The roles of nucleotide binding and hydrolysis at the proximal and distal nucleotide binding sites of UvrA were delineated by carrying out the cross-linking experiments with proteins harboring ATPase active site mutations.

We expected that the extent of disulfide bond formation between different cysteine pairs designed based on the 'open dimer' and 'closed dimer' conformations of UvrA in the presence of different nucleotides and DNA substrate would inform how ATP binding and hydrolysis affect UvrA conformational changes and how these changes might be used for the discrimination of damaged from undamaged DNA. Biochemical and structural characterization of the UvrA dimer 'trapped' in 'open dimer' and 'closed dimer' states would provide insights into the importance of conformational cycling in DNA damage recognition and repair. Conformation-specific disulfides designed based on the method described above (Craig and Dombkowski, 2013; Dombkowski, 2003) have been successfully used to study structural changes in several different proteins including transcription-repair coupling factor (Deaconescu et al., 2012), RNA polymerase (Ma et al., 2005), transcription factor (Laptenko et al., 2006), and transport proteins (Seeger et al., 2008; Sjoelund and Kaltashov, 2007).

4.2 Objective 2: To study the properties of UvrB dimer, and whether the UvrB dimer plays a role in selection of the damaged DNA strand for repair

Crystal structure of the UvrA•UvrB complex suggests involvement of two UvrB molecules in initial lesion recognition. Biochemical (Hildebrand and Grossman, 1999; Moolenaar et al., 2005), and more recently structural (Webster et al., 2012) studies also suggest that UvrB could form dimer in solution. However, the significance of UvrB dimer in solution has not been elucidated.

In our prior work with *Geobacillus stearothermophilus (Bst)* UvrB ortholog, we found that *Bst*UvrB forms stable dimer in solution, and that the dimer can be separated from monomer by gel filtration chromatography (Figure 3A).

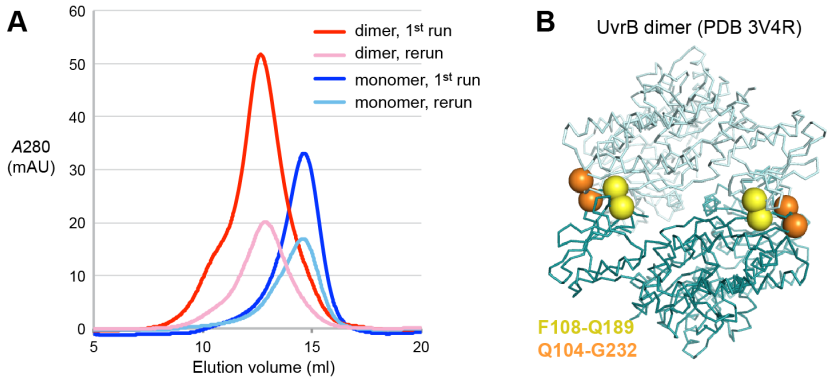

Figure 3 The UvrB 'dimer'. (A) *Bst*UvrB forms stable dimer that can be isolated from UvrB monomer. **(B)** Designed disulfide based on *B. subtilis* UvrB crystal structure

In order to investigate the functional significance of the observed UvrB dimer, and to determine whether the observed dimer is representative of the UvrB dimer formed during DNA lesion recognition, we proposed to purify and characterize the *Bst*UvrB dimer by measuring its ATP binding, ATPase, and DNA binding activities, in comparison with those of the well-characterized UvrB monomer. In addition, we proposed to investigate the role of UvrB dimer-monomer transition in NER by subjecting a disulfide-trapped UvrB dimer to UvrC-mediated incision assay. Disulfide-trapped UvrB would be designed in the same way as those described for UvrA (section 4.1), using the crystal structure of *Bacillus subtilis* UvrB dimer (PDB 3V4R), which displays 98.8% sequence identity to the *Bst* ortholog, as the starting model (Figure 3B). If we are able to determine the crystal structure of the *Bst*UvrB dimer, disulfide trapping could also be designed based on the new crystal structure.

We expected that the biochemical characterization of purified UvrB dimer would provide insights into the effects of monomer-dimer equilibrium of UvrB on its functions. Although other studies have described some preliminary analysis of UvrB dimer (Hildebrand and Grossman, 1999; Moolenaar et al., 2005; Verhoeven et al., 2002; Webster et al., 2012), the UvrB 'dimer' in all previous studies was **not** purified and was present as a mixture of dimer and monomer. With the stable *Bst*UvrB dimer, we would be able to characterize the pure preparation of UvrB dimer. Structural studies of the purified UvrB dimer could reveal whether the previously reported crystallographic UvrB dimer (PDB 3V4R, (Webster et al., 2012)) is representative of UvrB in solution or whether it was a result of crystal packing artifact. Understanding the properties of UvrB dimer, in comparison to those of the monomer, would provide insights into the function of two UvrB molecules in DNA damage recognition.

5. RESULTS

5.1 Expression and purification of UvrA cysteine mutants

Eight UvrA cysteine mutants were successfully expressed and purified: A59C, A61C, P81C, S91C, E133C, H750C, F751C, and R769C. In addition, we also expressed and purified wild-type UvrA, as well as two DNA binding mutants, R708A and K718A (Pakotiprapha et al., 2012) to be used as controls in the biochemical experiments (Figure 4).

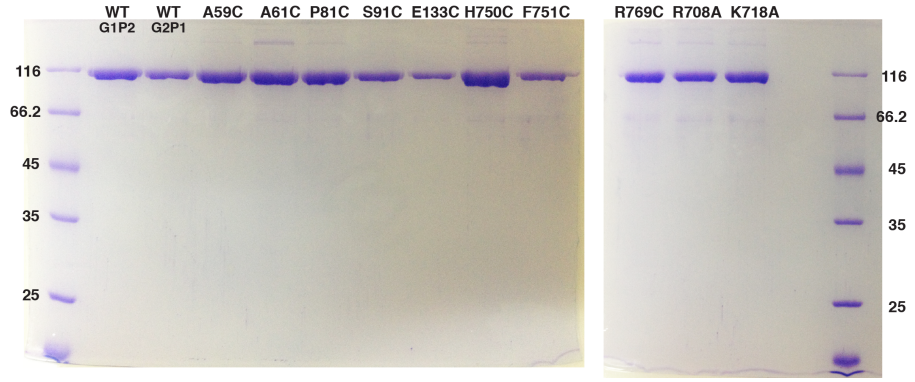

Figure 4 Purification of UvrA cysteine mutants. *Geobacillus stearothermophilus* UvrA (wild-type and mutants) were purified to ≥95% purity as judged by SDS-PAGE.

5.2 All UvrA cysteine mutants have intact ATPase and DNA binding activities

Due to instrument limitations, we needed to make modifications to the existing protocols for both the ATPase assay and the DNA binding assay. After several rounds of optimization, we were able to develop new experimental procedures to assay for the ATPase and DNA binding activities, and confirmed that all UvrA cysteine mutants are not impaired in ATP hydrolysis and DNA binding (Figures 5 and 6).

As seen in Figure 5, all UvrA mutants have ATPase activity that can be stimulated by DNA. In the absense of DNA, the turnover number (k_{cat}) ranges from 6–24 mol ATP/min/mol UvrA. Addition of DNA stimulated the ATPase activity by 7–13 fold, with the exception of R708A, which showed no stimulation; this is consistent with previous report that R708A mutant does not bind DNA (Pakotiprapha et al., 2012).

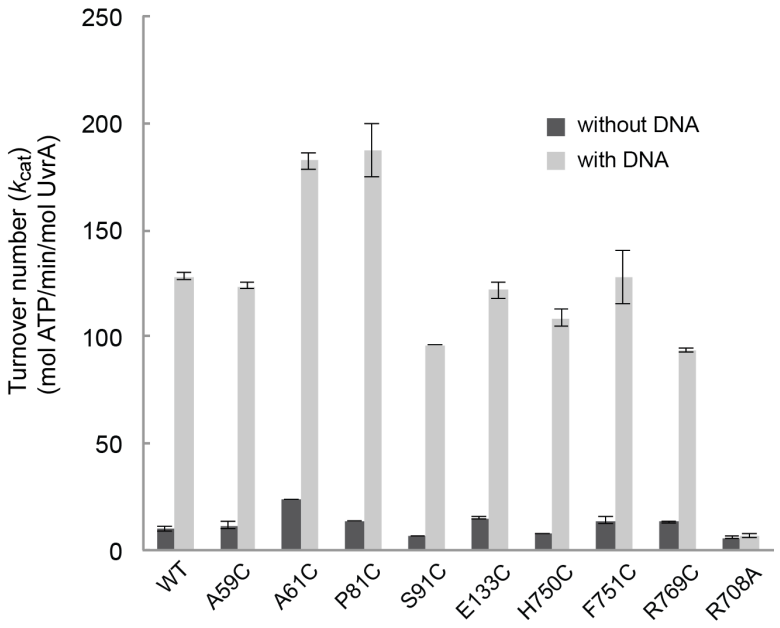

Figure 5 UvrA cysteine mutants have intact ATPase activity. ATP hydrolysis by UvrA was monitored by the coupled enzyme system consisting of pyruvate kinase and lactate dehydrogenase. The data were reported as mean turnover number (k_{cat}, mol ATP/min/mol UvrA) ± standard error (n = 3).

DNA binding activity of UvrA was assessed by titrating 20 nM five-nucleotide-mismatched DNA ((Zou et al., 1997) and personal communication with Brenowitz lab, Albert Einstein College of Medicine, New York, USA) with 0–200 nM UvrA. After 30-minute incubation at 55°C, the optimum temperature of *Bst*UvrA, the reactions were analyzed on 6% native polyacrylamide gel in the presence of 1 mM ATP and 10 mM $MgCl_2$. The gel was visualized by SYBR Gold fluorescence stain, and the band intensities were quantified. As seen in Figure 6, all cysteine mutants are capable of binding to DNA in a similar manner to wild-type UvrA.

The biochemical assays described above suggest that all eight UvrA cysteine mutants are not impaired in DNA binding and DNA-stimulated ATP hydrolysis, and can be used in disulfide crosslinking studies.

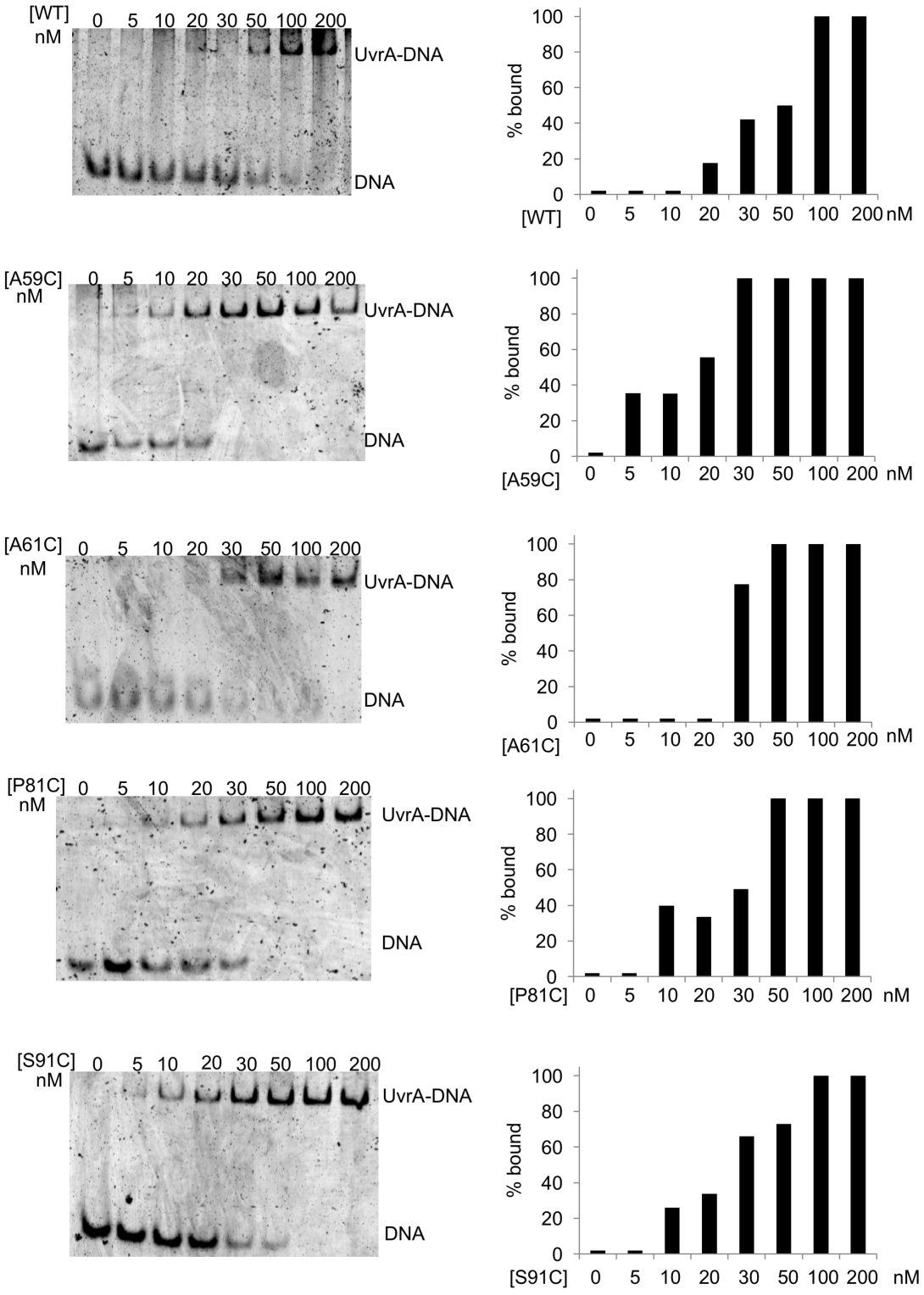

Figure 6 UvrA cysteine mutants have intact DNA-binding activity. DNA binding activity of UvrA was assessed by titrating 20 nM five-nucleotide mismatched DNA with 0–200 nM UvrA. The gel was visualized by SYBR Gold fluorescence stain (left), quantified, and presented as percent DNA bound at different protein concentrations (right).

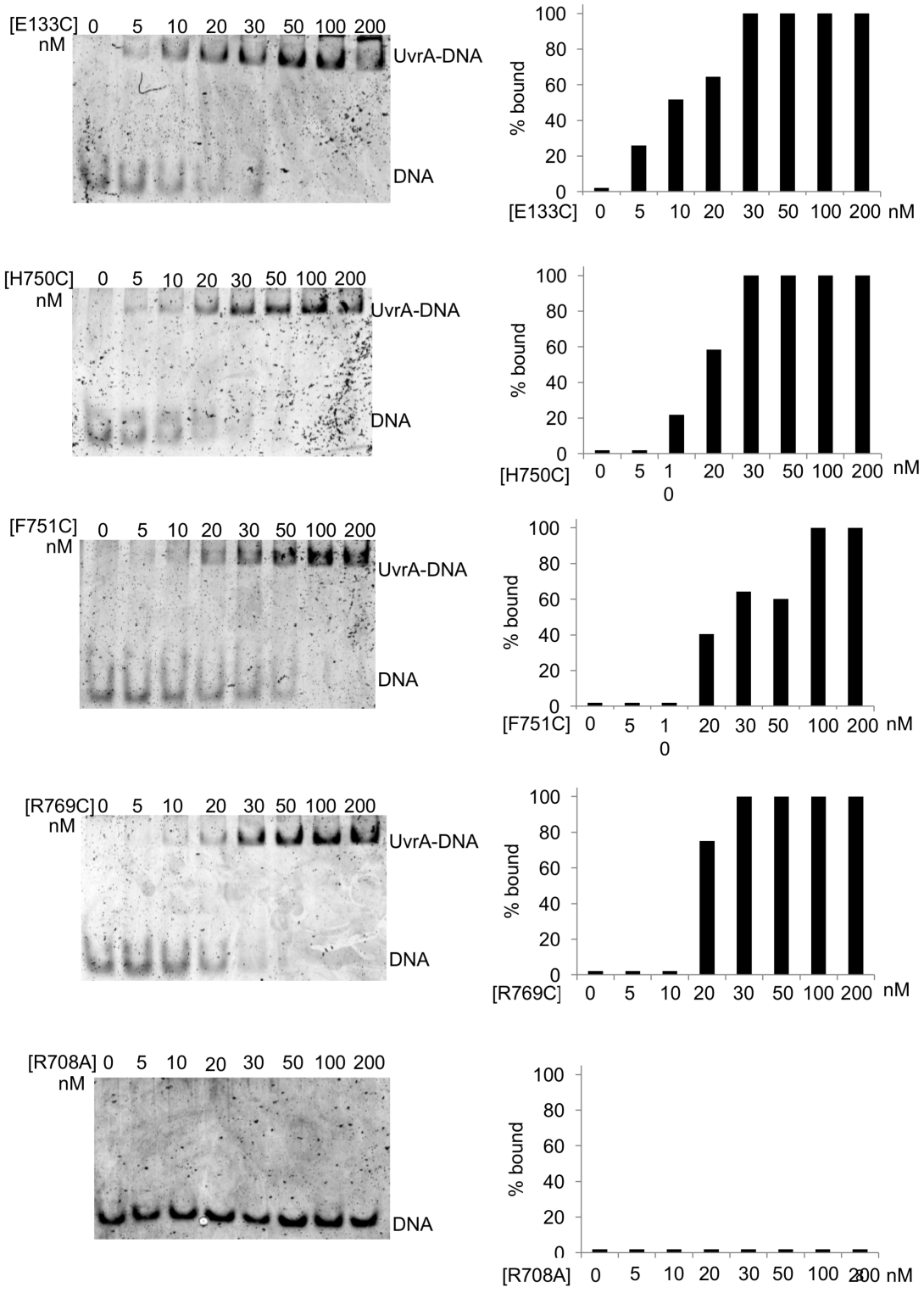

Figure 6 UvrA cysteine mutants have intact DNA-binding activity (continued). DNA binding activity of UvrA was assessed by titrating 20 nM five-nucleotide mismatched DNA with 0–200 nM UvrA. The gel was visualized by SYBR Gold fluorescence stain (left), quantified, and presented as percent DNA bound at different protein concentrations (right).

5.3 Crosslinking studies of UvrA in the 'open dimer' and 'closed dimer' conformations

As described in section 4.1, four cysteine pairs were predicted to form inter-molecular disulfide bond when UvrA is in the 'open dimer' conformation: P81C-P81C, H750C-H750C, A59C-S91C, and A61C-F751C. Of these, we initially chose two pairs for preliminary crosslinking studies: P81C-P81C and H750C-H750C. The reasons for choosing these two pairs are as follow: 1) the predicted disulfides do not require heterodimerization between two different cysteine mutants, which would simplify experimental setup; and 2) the energy function calculated from the torsion and bond angles of disulfides (Craig and Dombkowski, 2013; Dombkowski, 2003) involving P81C-P81C and H750C-H750C, 1.71 and 2.43 kcal/mol, respectively, is in the same range as that of native disulfide bonds. Ninety percent of native disulfides have an energy value less than 2.2 kcal/mol (Craig and Dombkowski, 2013), whereas the energy calculated from A59C-S91C and A61C-F751C are 8.48 and 3.45 kcal/mol, respectively.

UvrA cysteine mutants were incubated under non-reducing conditions to allow disulfide formation. Crosslinking reactions were set up in the presence or absence of nucleotides (ADP or ATP), DNA (undamaged or damaged), and UvrB. Representative results of the crosslinking reactions are shown in Figures 7A and 7B. Crosslinking reactions were also set up with wild-type UvrA to verify that the thirteen native cysteine residues of UvrA do not form any intermolecular disulfide bond (Figure 7C).

We found that the H750C-H750C crosslinking site gave very high crosslinking efficiency (70–90%) in the absence of DNA. When DNA was added, crosslinking efficiency is substantially reduced. In the presence of nucleotide, however, crosslinking efficiency is high regardless of whether DNA was present (Figures 7A and 7B). Several types of 'damaged' DNA were used in the crosslinking assays including UV-irradiated plasmid (Biggerstaff and Wood, 2006; Kovalsky and Grossman, 1998; Orren and Sancar, 1989, 1990), 50-mer dsDNA containing single-nucleotide gap (DellaVecchia et al., 2004; Moolenaar et al., 2001), and 50-mer fluorescein-containing DNA (Skorvaga et al., 2002). All DNA lesions that were tested gave similar results (data not shown).

Our crosslinking results are consistent with the the observation that the binding of DNA to UvrA causes the β-hairpin of the signature domain II of the two UvrA protomers, on which H750C is located, to move away from each other (PDB 3PIH (Jaciuk et al., 2011), see also section 5.4). We propose that ATP increases the

dynamics of DNA binding by UvrA, and could play a role in DNA damage recognition by allowing UvrA to dissociate from undamaged sites.

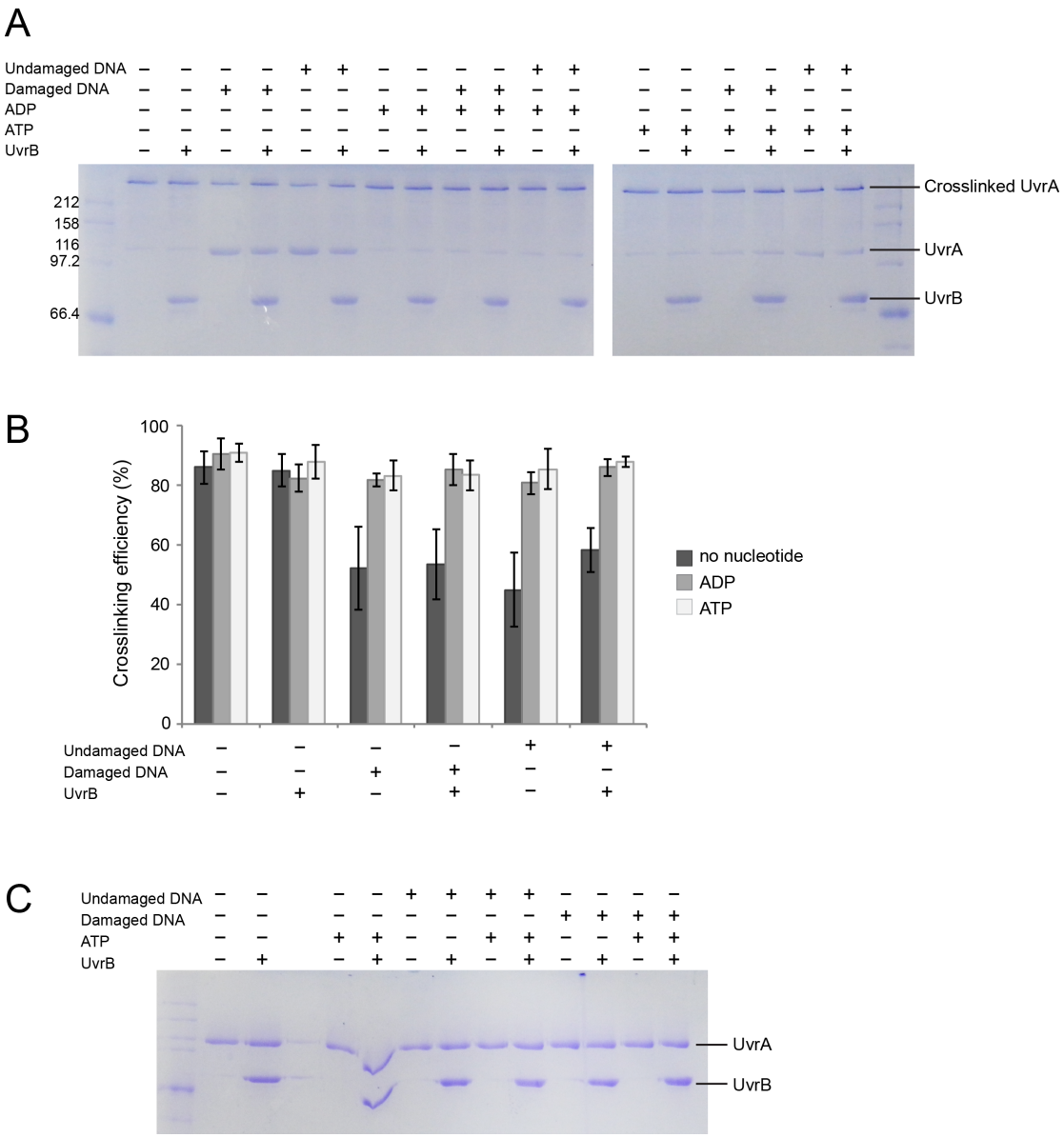

Figure 7 Crosslinking of UvrA in the 'open dimer' conformation. **(A)** SDS-PAGE analysis of crosslinking reactions at the H750C-H750C crosslinking site after 24-hour incubation. Undamaged and damaged DNA were linearized pUC19 and linearized pUC19 that had been irradiated with UV, respectively. **(B)** Quantification of band intensities. The data were reported as the mean percent crosslinking ± standard error (n = 3) **(C)** SDS-PAGE analysis of crosslinking reactions of wild-type UvrA confirmed that the thirteen native cysteine residues do not form disulfide crosslinking under our experimental conditions.

The P81C-P81C crosslinking site, which also represent the 'open dimer' conformation of UvrA, gave complicated pattern of higher-molecular weight bands across all conditions (data not shown). Since replacement of proline residue could potentially affect structural stability of the protein, we decided not to pursue this crosslinking site further, and instead focused our efforts on the H750C-H750C crosslinking site, which behaved well in preliminary experiments.

For the 'closed dimer' conformation, only one pair of disulfide was predicted: E133C-R769C. Crosslinking studies were carried out as described for the 'open dimer' conformation and the results are shown in Figure 8.

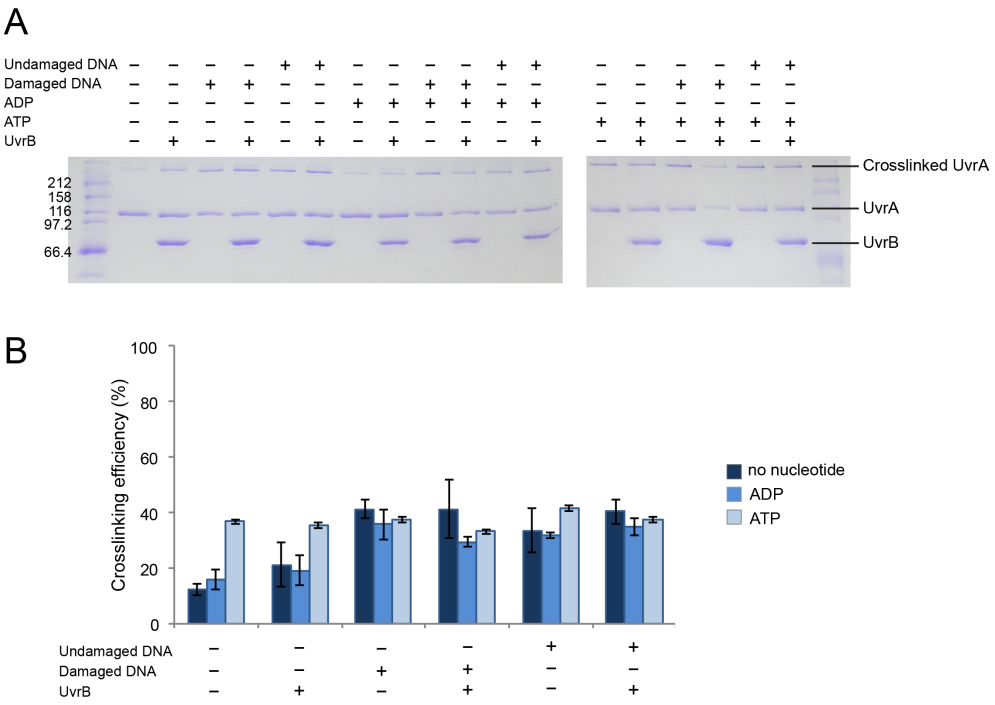

Figure 8 Crosslinking of UvrA in the 'closed dimer' conformation. (A) SDS-PAGE analysis of crosslinking reactions at the E133C-R769C crosslinking site after 24-hour incubation. Undamaged and damaged DNA were linearized pUC19 and linearized pUC19 that had been irradiated with UV, respectively. **(B)** Quantification of band intensities. The data were reported as the mean percent crosslinking ± standard error (*n* = 3)

Overall, the crosslinking efficiencies in the 'closed dimer' conformation were much lower than in the 'open dimer' conformation (Figure 8). When linearized pUC19 was used as DNA substrate, crosslinking efficiency seems to be higher in the presence of DNA, and addition of ATP, but not ADP, increased crosslinking efficiency in the absence of DNA (Figure 8B). However, these results were not reproducible when 50-

mer model substrates containing single-nucleotide gap or fluorescein-dT were used (data not shown). In addition, we found that E133C mutant showed 10–20% crosslinking when present alone (data not shown). Due to the fact that the levels of crosslinking observed with E133C alone is similar to those with E133C-R769C mixtures, and that the results obtained with different DNA substrates were variable, we were not able to draw conclusions from crosslinking studies in the 'closed dimer' conformation.

Although we were not able to use disulfide crosslinking assays to study the roles of the transition between 'open dimer' and 'closed dimer' conformations of UvrA in DNA damage recognition, the observation that crosslinking at the H750C-H750C site is dramatically influenced by the presence of DNA and ATP suggested that the β-hairpin of the signature domain II of UvrA, on which H750 is located, could play a crucial role in lesion recognition, and that the movement of this hairpin is likely regulated by ATP binding and hydrolysis.

5.4 Trapping of the β-hairpin of the third zinc-binding module (Zn3hp) in the 'closed' conformation'

UvrA possesses three Zn modules, which are not found in other proteins in the ATP-binding cassette (ABC) superfamily of ATPases (Doolittle et al., 1986; Pakotiprapha et al., 2008). The third Zn module, which is inserted into the signature domain II, contains a β-hairpin (Zn3hp).

Previous study showed that deletion of Zn3hp increased DNA binding ability (Croteau et al., 2006; Wagner et al., 2011). However, this mutation attenuated UvrB loading and damage incision ability when undamaged DNA was added to the reaction as a competitor (Croteau et al., 2006). *In vivo* experiments in *Escherichia coli* also revealed that deletion of Zn3hp rendered the bacteria very sensitive to UV (Croteau et al., 2006; Wagner et al., 2011).

Based on these observations, Zn3hp has been proposed to play a crucial role in damage recognition. However, since previous studies were done using 'ZnG' mutants, in which the entire Zn3hp was deleted, no information is currently available on how Zn3hp changes conformation during lesion recognition, and how such changes are regulated.

To better understand the role of Zn3hp movement during DNA damage recognition, the movement of Zn3hp was restricted by disulfide crosslinking using the H750C-H750C crosslinking site. Structural analysis revealed that in the absence of DNA, H750 from each UvrA protomer is located close to each other at the dimer

interface (‘closed’ conformation of Zn3hp, Figures 9B and 9C), whereas in the presence of DNA, the two H750 residues are far apart (‘open’ conformaiton of Zn3hp, Figure 9A and 9C). By trapping the Zn3hp in the ‘closed’ conformation using disulfide crosslinking at the H750C-H750C site, we should be able to gain insights into whether the transition between the ‘closed’ and ‘open’ conformation of Zn3hp is required for damage recognition. To prepare the crosslinked protein, H750C mutant was incubated under non-reducing condition at room temperature for 24 hours. The protein used in subsequent biochemical assays was crosslinked to about 80% (Figure 9D), unless stated otherwise.

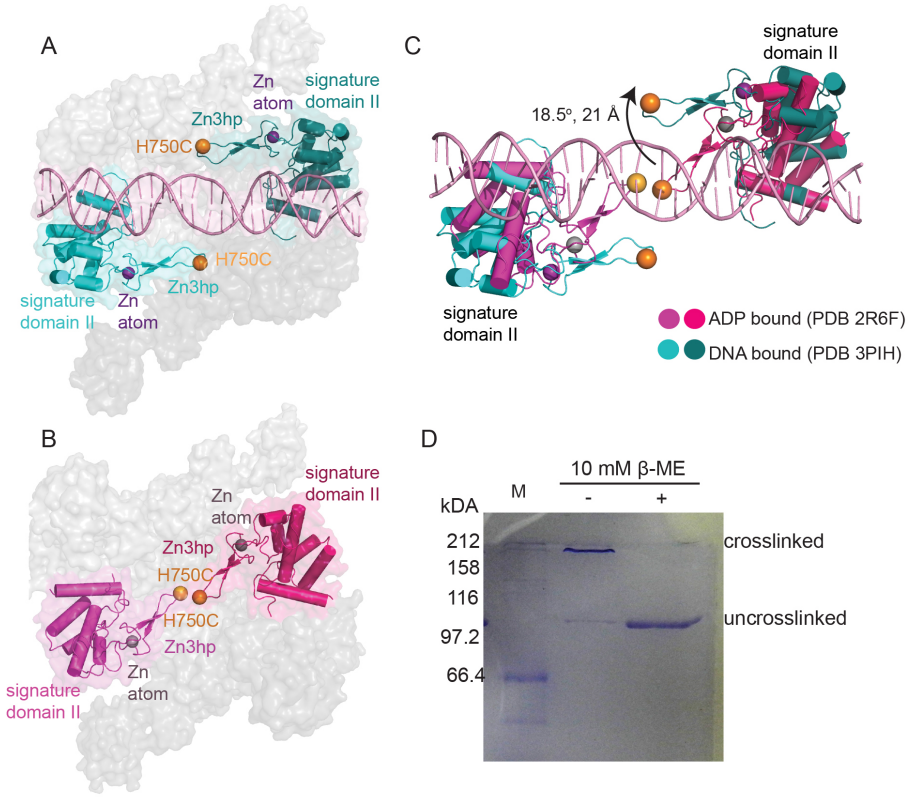

Figure 9 Conformational change of signature domain II and Zn3hp upon DNA binding. **(A)** UvrA-DNA complex (PDB 3PIH). **(B)** UvrA-ADP (PDB 2R6F). **(C)** UvrA-DNA complex (PDB 3PIH) was superposed on UvrA-ADP (PDB 2R6F) using the positions of C_α of the two ATP-binding domains. Superposition indicates the 18.5° rotation of signature domain II to accommodate the DNA; this causes the tip of Zn3hp to be ~21 Å apart. **(D)** Crosslinked H750C analysis by non-reducing SDS-PAGE. The crosslinking efficiency was about 80%.

5.5 Conformational change of Zn3hp is crucial for damage-specific DNA binding.

To investigate whether DNA binding requires the movement of Zn3hp, the DNA-binding capacity of the crosslinked protein was examined using EMSA under various UvrA concentrations. Crosslinking disrupted the binding between UvrA and damaged DNA, however, it did not affect binding to undamaged DNA (Figure 10).

Since the dissociation constant for binding between *Geobacillus stearothermophilus* UvrA and damaged DNA is approximately 0.5 nM (Pakotiprapha et al., 2012) and UvrA binds to DNA as a dimer, the 20 nM damaged DNA substrate in the assay was expected to be completely bound when UvrA monomer concentration was 40 nM or higher. In the crosslinked state, UvrA formed complex with <50% of damaged DNA at 50 nM monomer concentration (Figures 10A and 10C). In contrast, when crosslinking was removed by adding β-ME, >80% of the damaged DNA was bound in the reaction with 50 nM monomer (Figures. 10B and 10C). The different percentage of complex formed by crosslinked and uncrosslinked UvrA in the presence of damaged DNA was observed at UvrA concentrations between 5–50 nM (Figure 10C). This clearly shows that the crosslink impairs the ability of UvrA to bind to the damaged DNA. Complete binding of damaged DNA was, however, observed when UvrA concentration was greater than 100 nM under both crosslinked and uncrosslinked conditions. This could be due to complex formation between damaged DNA and the ~20% of UvrA that remained uncrosslinked (Figure 9D). For undamaged DNA, the percentages of UvrA-DNA complex formed by crosslinked and uncrosslinked protein were comparable (Figures 10D–10F).

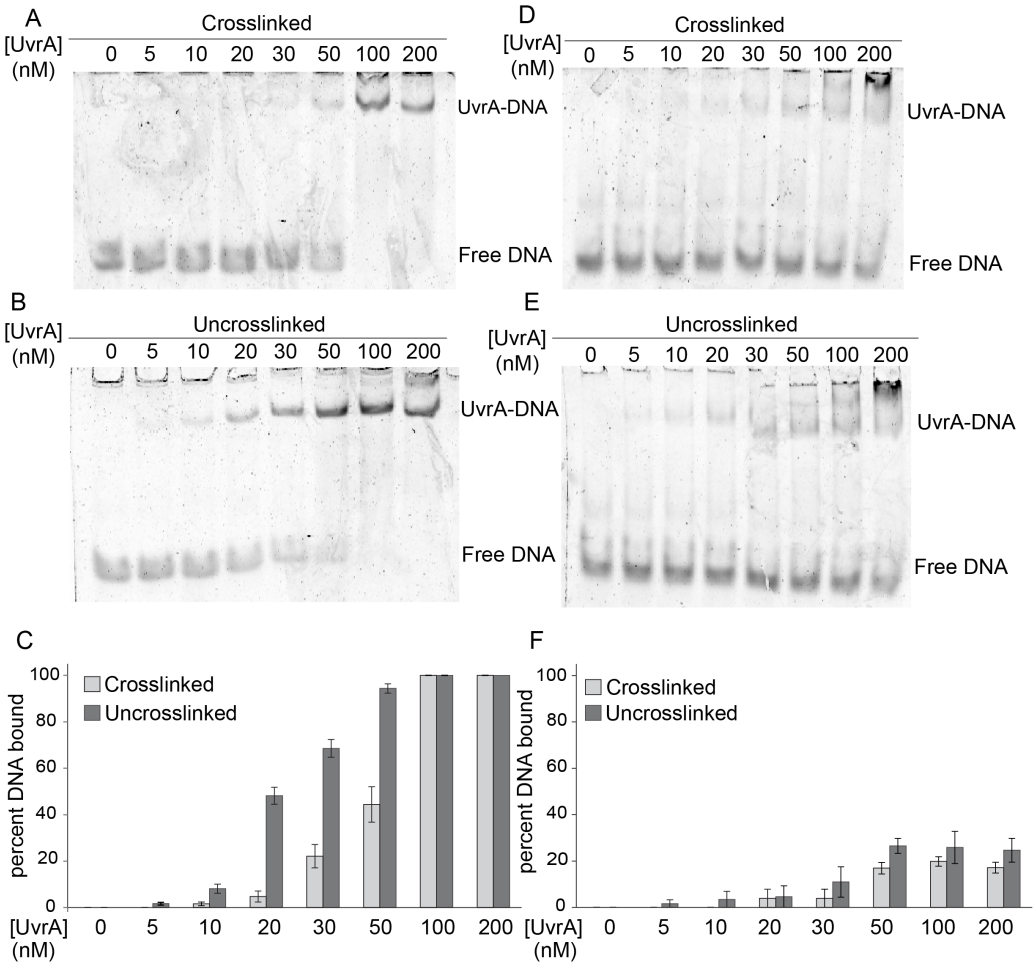

Figure 10 The movement of Zn3hp is required for damage-specific binding. DNA binding ability of crosslinked and uncrosslinked UvrA was assay using EMSA by titrating 20 nM DNA substrate with 0–200 nM UvrA. **(A)** Damaged DNA binding by H750C-H750C crosslinked UvrA. **(B)** Damaged DNA binding by H750C UvrA that had been uncrosslinked by addition of β-ME. **(C)** Quantitative analysis of panels (A) and (B). **(D)** Undamaged DNA binding by H750C-H750C crosslinked UvrA. **(E)** Undamaged DNA binding by H750C UvrA that had been uncrosslinked by addition of β-ME. **(F)** Quantitative analysis of panels (D) and (E). The data are reported as mean ± standard error (*n*=3).

5.6 Movement of Zn3hp is required for UvrB loading

In addition to the DNA damage detection, another role of UvrA is to deliver UvrB onto the DNA lesion to form a pre-incision complex (Kacinski and Rupp, 1981; Van Houten et al., 1987). Within the pre-incision complex, the lesion is verified by UvrB. Subsequently, UvrC is recruited and the damage incision occurs (Moolenaar et al., 2000; Seeley and Grossman, 1990). The DNA binding assay revealed that the crosslinked UvrA is impaired in damage sensing. We next assessed whether the crosslinked UvrA can load UvrB onto the damaged site.

To test UvrB loading ability of the crosslinked protein, the pre-incision complex formation was analyzed using EMSA. We found that the UvrB-DNA complex formation dramatically decreased when the crosslinked UvrA was used in the reaction. However, when the disulfide linkage was reversed by the addition of β-ME, the UvrB loading activity of UvrA was restored (Figures 11A–C). This shows that the restriction of Zn3hp movement disrupts UvrB loading, which is the downstream process of DNA damage detection.

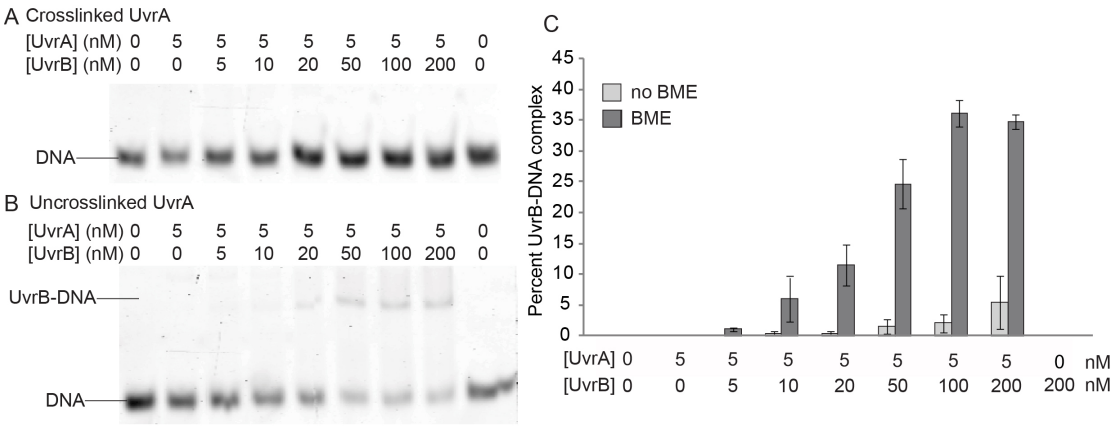

Figure 11 The restricted movement of Zn3hp disrupts UvrB loading activity. UvrB loading by **(A)** crosslinked UvrA and **(B)** uncrosslinked UvrA, as judged by EMSA. **(C)** Percent of UvrB-DNA complex formation. The data are reported as mean ± standard error (*n*=3).

5.7 Movement of Zn3hp is essential for ATP hydrolysis

Having shown that the movement of the Zn3hp is required for the damage-specific DNA binding and the UvrB loading activities of UvrA, we further investigated whether the switch between the open and closed conformations of Zn3hp is also required for the ATP hydrolysis, which is required for the initial steps of NER. The ATPase activity of UvrA was measured using a coupled-enzyme assay system consisting of pyruvate kinase and lactate dehydrogenase, in which ATP hydrolysis is coupled to oxidation of NADH (Kiianitsa et al., 2003; Lindsley, 2001). Since the ATPase activity of UvrA from *Geobacillus stearothermophilus* is stimulated by DNA (Pakotiprapha et al., 2008), we performed the ATPase assay both in the presence and absence of DNA.

The crosslinked UvrA cannot hydrolyze ATP either in the presence or absence of DNA. The result showed 50% drop in the ATPase activity of the crosslinked UvrA compared to the activity of the uncrosslinked protein. The percentage of the decreased ATPase activity was proportional to the 50% crosslinked UvrA used in the assay (Figure 12). When crosslinking was removed by the addition of a reducing agent, the ATPase activity of protein was restored and the rate of reaction was comparable to that of the wild-type UvrA. This led us to conclude that crosslinking abolishes the ATPase activity of UvrA, and that all the remaining activity observed under the crosslinked condition was due to the uncrosslinked population.

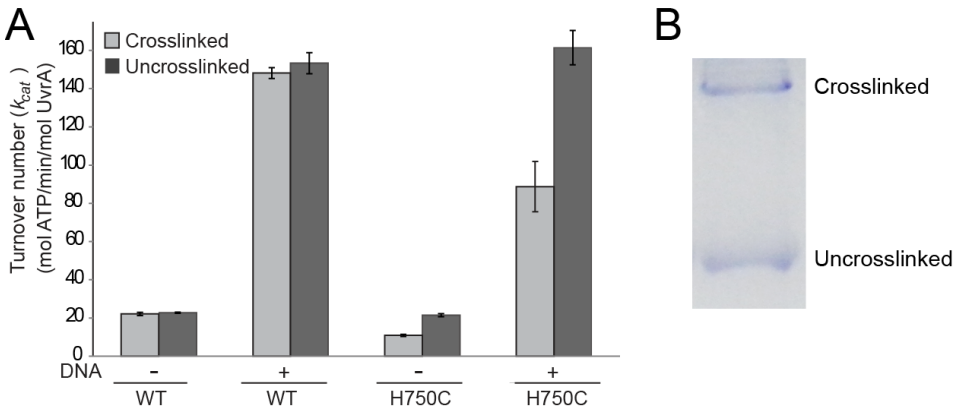

Figure 12 The movement of Zn3hp is required for ATP hydrolysis. (A) Average turnover number of ATP hydrolysis by wild-type and H750C UvrA. The data are reported as mean turn over number (mol ATP/min/mol UvrA) ± standard error (*n*=3). **(B)** The 'crosslinked' protein sample was crosslinked to ~50%.

Overall, our results indicate that the movement of the Zn3hp and ATP hydrolysis are coupled. The ATP hydrolysis activity of UvrA was lost by restricting the movement of the β-hairpin, and can be rescued by severing the disulfide linkage. The loss of the ATPase activity when a conformational change at a site distant from the ATPase active site was restricted was also observed in Msh2-Msh6, another member of the ABC family (Hargreaves et al., 2012). Msh2-Msh6 complex couples ATP hydrolysis to a conformational change within its C-terminal region. When the conformational change was prevented using disulfide crosslinking, Msh2-Msh6 has low affinity for ATP and exhibit the loss-of-function phenotype.

5.8 ATP hydrolysis at the distal nucleotide binding site mediates the movements of Zn3hp

Conformational changes in UvrA were proposed to be involved in the early steps of NER and be triggered by DNA substrates, UvrB, and ATP (Goosen and Moolenaar, 2001; Pakotiprapha et al., 2012; Rossi et al., 2011). To investigate whether these factors affect the conformational change of Zn3hp, we measured the crosslinking efficiency of UvrA in the presence and absence of UvrB, ATP, damaged and undamaged DNA.

Similar to other ABC proteins, UvrA couples ATP hydrolysis to conformational change. Crosslinking analysis showed that both DNA and ATP hydrolysis affect the switching between the open and closed conformations of the Zn3hp. The presence of DNA reduced percentage of crosslinking to about 50% (Figure 13A). This result is consistent with the structure of the UvrA-DNA complex (Figure 9A), which suggests that the Zn3hp needs to rotate away from each other to accommodate the DNA (Jaciuk et al., 2011). However, when ATP was added to the reaction, the crosslinked population increased to 90% regardless of DNA presence. This is consistent with the ADP-bound structure in which the Zn3hp from each protomer are in close proximity (Figure 9B) (Pakotiprapha et al., 2008).

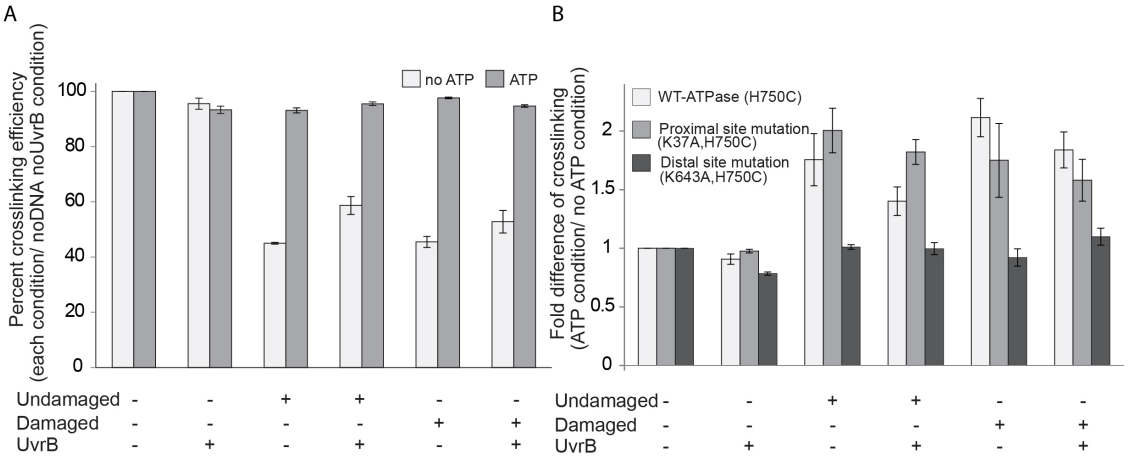

Figure 13 ATP binding/ ATP hydrolysis at distal site controls the conformational change between open and closed β-hairpin. (A) The conformational change of Zn3hp during damage recognition event in presence of different factors (damaged and undamaged DNA, UvrB, and ATP). The data are represented as mean percent crosslinking ± standard error (*n*=5). **(B)** Comparison of the effect of ATP on β-hairpin movement in ATPase-wild type UvrA and active site mutants. The data are represented as mean fold difference ± standard error (*n*=5).

UvrA possesses two non-identical nucleotide binding sites, designated as proximal and distal sites, respectively (Pakotiprapha et al., 2008). The exact role of each nucleotide binding site is still controversial. Studies of two single-site *E.coli* mutants showed that both mutants are deficient in damage repair *in vivo* (Myles et al., 1991; Thiagalingam and Grossman, 1991; Wagner et al., 2010). Sancar and colleagues showed that although both ATPase mutants can bind damaged DNA, their UvrB-loading activity was dramatically reduced (Myles et al., 1991). However, evidence from the Grossman group revealed that only the distal site mutant lost the damage incision ability, while the proximal site mutant was still able to initiate damage incision (Thiagalingam and Grossman, 1991). On the other hand, the result from the Goosen group showed that the efficiency of damage incision of the proximal site mutant was similar to wild-type. Although the distal site mutant could not repair the damage in a 50-bp DNA substrate, the repair ability was rescued by increasing the length of DNA (Wagner et al., 2010).

To investigate the involvement of each nucleotide binding sites in the movement of the Zn3hp, the ATPase activity of each ATP-binding sites was deactivated by substituting K37 and K643 in the walker A motive with alanine, respectively. Such alanine substitution mutation has been used to study other ATPases such as SMC

(Lammens et al., 2004), DMC1 (Sharma et al., 2013), ABC transporter BmrA (Orelle et al., 2008), and MalK transporter (Panagiotidis et al., 1993). This mutation is expected to abolish ATP binding at the mutated site. These mutants have drastically reduced ATPase activities (Figure 14), consistent with previous studies (Myles et al., 1991; Thiagalingam and Grossman, 1991; Wagner et al., 2010).

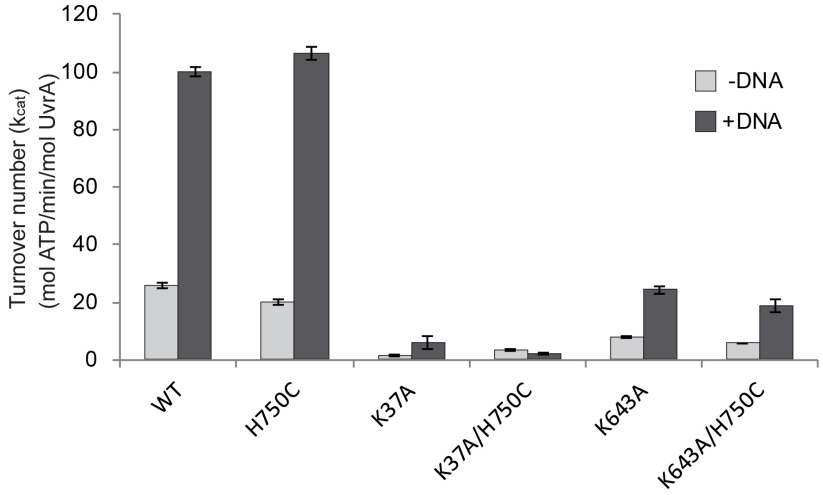

Figure 14 ATP hydrolysis by ATPase wild-type and mutant UvrA . K37A and K643A represent alanine substitution of the conserved lysine residue in the Walker A motif of the proximal and distal nucleotide binding site, respectively. The data are reported as mean turnover number (mol ATP/min/mol UvrA) ± standard error (*n*=3).

Similar to the ATPase wild-type (H750C), ATP increases the crosslinking efficiency of the proximal site mutant by about two folds in DNA-containing conditions (Figure 13B). In contrast, the crosslinking of the distal site mutant in the presence of DNA was not restored by the addition of ATP. Therefore, it appears that mutation at the distal site either prevents the Zn3hp from adopting the closed conformation, or abolishes movement of the Zn3hp.

Our finding revealed that the ATP binding/hydrolysis at the distal site regulates the movement of Zn3hp. This result is supported by the previous studies of the distal site mutant in which this mutation appeared to reduce UvrB loading (Wagner et al., 2010) and incision activities (Thiagalingam and Grossman, 1991; Wagner et al., 2010). *In vivo* assays showed that the distal site mutation also abolished DNA repair process (Myles et al., 1991; Thiagalingam and Grossman, 1991; Wagner et al., 2010).

5.9 Characterization of the UvrB 'dimer'

Geobacillus stearothermophilus UvrB was expressed and purified from E. coli. The 'monomer' and 'dimer' fractions were then separated by size exclusion chromatography (Figure 3A) and subjected to biochemical and biophysical analyses. Both the monomer and dimer fractions exhibited virtually no ATPase activity in the absence of UvrA, consistent with prior results. Their DNA-binding activities are also indistinguishable (Figure 15).

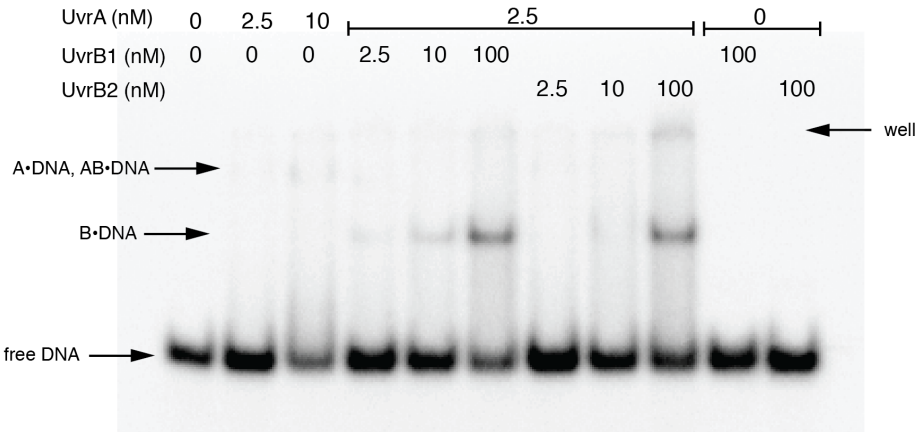

Figure 15 DNA binding properties of UvrB 'momoner' and 'dimer' fractions. UvrB 'monomer' and 'dimer fractions were subjected to UvrB loading assay. UvrB1 and UvrB2 designate the monomer and dimer fractions, respectively.

Further analysis using analytical centrifugation at various UvrB concentrations revealed that both the 'monomer' and 'dimer' fractions have apparent molecular weight close to that of UvrB monomer (data not shown). Fluorescence spectroscopy measurement suggested that what was previously thought of as the UvrB 'dimer' fraction is likely UvrB monomer in complex with a sub-stoichiometric contaminant with high tryptophan content (Brenowitz, personal communication). The identity of this contaminant remains elusive as its amount is too low to be reliably detected by SDS-PAGE. We have attempted to analyze the 'dimer' fraction by mass spectrometry but failed to identify any protein other than UvrB. Based on these observation, we decided not to pursue further studies of UvrB oligomers and focus our efforts on UvrA.

6. CONCLUSION AND DISCUSSION

6.1 UvrA uses different DNA binding modes to interact with DNA

DNA binding assays showed different levels of binding to damaged DNA when crosslinked and uncrosslinked UvrA was used. However, no difference was observed in the binding between undamaged DNA and both types of UvrA (Figure 10).

We proposed that UvrA employs two different DNA binding modes to locate DNA lesions (Figure 16). During an initial Zn3hp-independent phase, UvrA might interact with both damaged and undamaged DNA through electrostatic interactions using residues around its DNA binding path. These residues are located on the signature domain II, signature domain I, insertion domain, and the first and second Zn binding modules (Pakotiprapha et al., 2012). Previous studies showed that mutation of the positively charged residues in the signature domain II (Pakotiprapha et al., 2008; Pakotiprapha et al., 2012), the insertion domain (Pakotiprapha et al., 2012; Timmins et al., 2009; Wagner et al., 2011), and the cluster of residues the signature domain I and in Zn modules 1 and 2 (Pakotiprapha et al., 2012) disrupted DNA binding.

Upon damage recognition, UvrA switches to a Zn3hp-dependent mode of binding that relies on the interaction between the lesion and the Zn3hp. We propose that the complex between the Zn3hp and the damaged DNA is stable while that between the Zn3hp and the undamaged DNA is not. The conformational change in the Zn3hp is indispensable for initiating the Zn3hp-dependent binding mode.

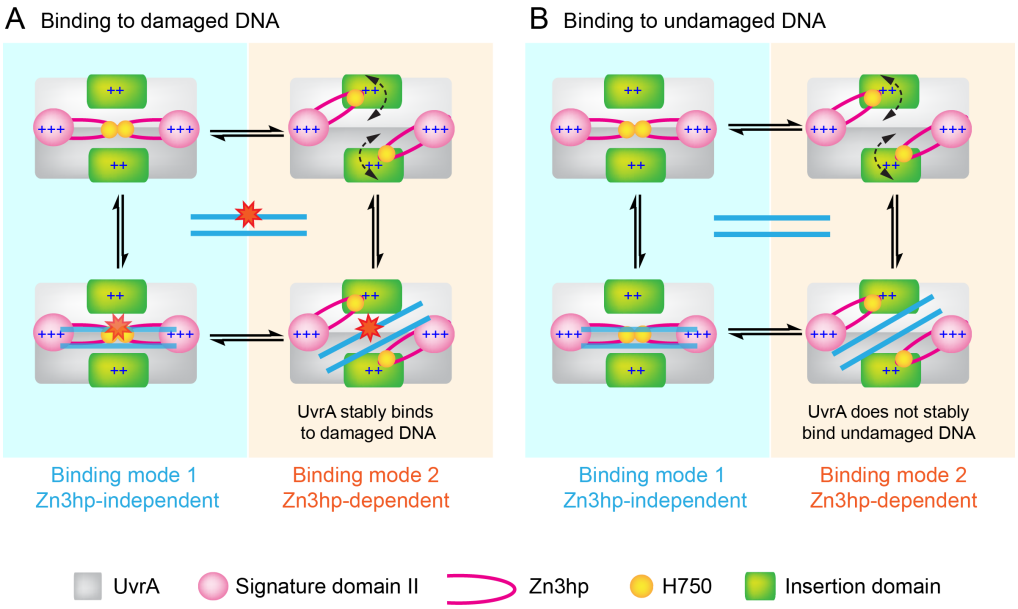

Figure 16 Model for lesion recognition by UvrA.

The model is well supported by our result. The apparent difference between the binding of damaged DNA with the crosslinked and the uncrosslinked protein indicated that, unlike the uncrosslinked UvrA which binds damaged DNA using both DNA binding modes, the crosslinked UvrA can only interact with damaged DNA using electrostatic interaction since the crosslinking makes the tip of the hairpin inaccessible to DNA. In addition, since electrostatic interactions occur during the initial binding with all types of dsDNA, there was no difference between binding of undamaged DNA with crosslinked and uncrosslinked protein.

The importance of Zn3hp for damage binding was also supported by EMSA performed on other Zn3hp mutants. When residues at the tip of the hairpin (M749, H750, F751 and L752) were replaced by alanine, the mutant can bind equally well to undamaged DNA compared to the wild-type which preferentially bind damaged DNA, however, it can bind to damaged DNA with slightly lower affinity than the wild type (Figure 17).

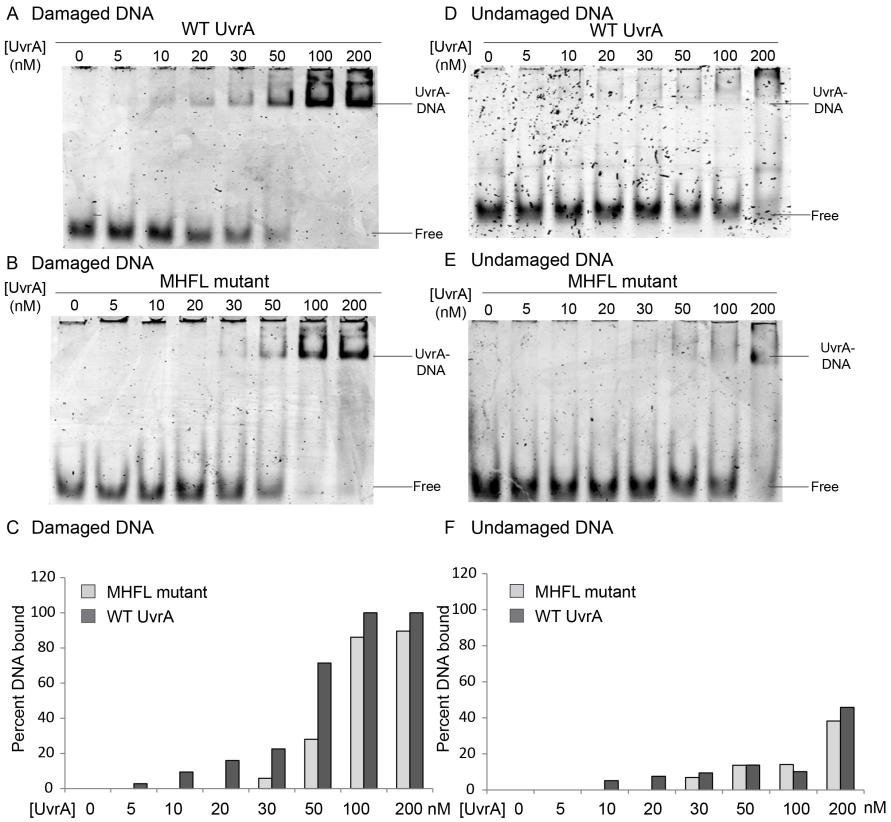

Figure 17 DNA binding ability of Zn3hp mutant was lower than wild-type UvrA. Four residues at the tip of Zn3hp were mutated to alanine: M749A/H750A/F751A/L752A. DNA binding activity of the mutant was assessed by EMSA. The mutant was impaired in damage DNA binding; binding to undamaged DNA appeared unaffected.

6.2 ATP hydrolysis at the distal site increases the dynamics of the Zn3hp

We proposed that ATP binding and hydrolysis at the distal site increases the dynamics of the Zn3hp such that the hairpins sample the open and closed conformations at an accelerated rate. In the WT-ATPase (H750C) and the proximal site mutant, ATP significantly increased the percentage of crosslinking in the presence of both damaged and undamaged DNA. In contrast, such effect was not observed in the distal site mutant (Figure 13). In the assays, ATP would interact with UvrA at a faster rate than DNA as diffusion rates are inversely proportional to molecular weights and the ATP concentration was approximately 10^4-fold higher than that of DNA. Once ATP hydrolysis at the distal site occurs, it increases the dynamics of the Zn3hp and raises the propensity at which the tips of the hairpins would adopt the closed or crosslinked conformation. Accordingly, the addition of ATP to the distal site mutant did not alter the extent of crosslinking because of the lack of ATP hydrolysis

6.3. Conclusion

The specific disulfide crosslinking experiment provides insight into the role of conformational change of the β-hairpin of the third Zn-binding module of UvrA (Zn3hp). The switch between the open and closed conformations of Zn3hp is essential for lesion recognition. The movement of Zn3hp is controlled by ATP hydrolysis at the distal nucleotide binding site, and is required for damage-sensing, ATP hydrolysis and UvrB loading, which is crucial for the initiation of damage verification and incision of NER.

7. OUTPUT (Acknowledge the Thailand Research Fund)

7.1 International Journal Publication

One munuscript is being prepared for submission:

Kraithong T*., Channgam K*., Tiensuwan M., Itsathitphaisarn O., Jeruzalmi D., and Pakotiprapha D. *Movement of β-hairpin in the third zinc-binding module of UvrA is required for DNA damage detection.*

*These authors contributed equally to this work.

The manuscript will be submitted to one of the following journals

Nucleic Acid Research	Impact Factor 9.112 (8.867)
DNA Repair	Impact Factor 3.333 (3.455)
Mutation Research	Impact Factor 3.015 (3.019)

Note: The numbers in parentheses are 5-year Impact Factor.

7.2 Application

–

7.3 Others

One proceeding has been published.

Channgam K. and Pakotiprapha D. *Expression, purification, and biochemical characterization of UvrA protein containing site-specific cysteine substitutions for monitoring of protein conformational change during DNA damage recognition.* The 10th International Symposium of The Protein Society of Thailand. 15-17 July 2015 Chulabhorn Research Institute.

8. REFERENCES

Biggerstaff, M., and Wood, R.D. (2006). Repair synthesis assay for nucleotide excision repair activity using fractionated cell extracts and UV-damaged plasmid DNA. Methods in molecular biology (Clifton, NJ *314*, 417-434.

Craig, D.B., and Dombkowski, A.A. (2013). Disulfide by Design 2.0: a web-based tool for disulfide engineering in proteins. BMC Bioinformatics *14*, 346.

Croteau, D.L., DellaVecchia, M.J., Wang, H., Bienstock, R.J., Melton, M.A., and Van Houten, B. (2006). The C-terminal zinc finger of UvrA does not bind DNA directly but regulates damage-specific DNA binding. The Journal of biological chemistry *281*, 26370-26381.

Deaconescu, A.M., Sevostyanova, A., Artsimovitch, I., and Grigorieff, N. (2012). Nucleotide excision repair (NER) machinery recruitment by the transcription-repair coupling factor involves unmasking of a conserved intramolecular interface. Proceedings of the National Academy of Sciences of the United States of America *109*, 3353-3358.

DellaVecchia, M.J., Croteau, D.L., Skorvaga, M., Dezhurov, S.V., Lavrik, O.I., and Van Houten, B. (2004). Analyzing the handoff of DNA from UvrA to UvrB utilizing DNA-protein photoaffinity labeling. The Journal of biological chemistry *279*, 45245-45256.

Dombkowski, A.A. (2003). Disulfide by Design: a computational method for the rational design of disulfide bonds in proteins. Bioinformatics *19*, 1852-1853.

Doolittle, R.F., Johnson, M.S., Husain, I., Van Houten, B., Thomas, D.C., and Sancar, A. (1986). Domainal evolution of a prokaryotic DNA repair protein and its relationship to active-transport proteins. Nature *323*, 451-453.

Goosen, N., and Moolenaar, G.F. (2001). Role of ATP hydrolysis by UvrA and UvrB during nucleotide excision repair. Research in microbiology *152*, 401-409.

Hargreaves, V.V., Putnam, C.D., and Kolodner, R.D. (2012). Engineered disulfide-forming amino acid substitutions interfere with a conformational change in the mismatch recognition complex Msh2-Msh6 required for mismatch repair. The Journal of biological chemistry *287*, 41232-41244.

Hildebrand, E.L., and Grossman, L. (1999). Oligomerization of the UvrB nucleotide excision repair protein of Escherichia coli. The Journal of biological chemistry *274*, 27885-27890.

Jaciuk, M., Nowak, E., Skowronek, K., Tanska, A., and Nowotny, M. (2011). Structure of UvrA nucleotide excision repair protein in complex with modified DNA. Nature structural & molecular biology *18*, 191-197.

Kacinski, B.M., and Rupp, W.D. (1981). E. coli uvrB protein binds to DNA in the presence of uvrA protein. Nature *294*, 480-481.

Kiianitsa, K., Solinger, J.A., and Heyer, W.D. (2003). NADH-coupled microplate photometric assay for kinetic studies of ATP-hydrolyzing enzymes with low and high specific activities. Analytical biochemistry *321*, 266-271.

Kovalsky, O.I., and Grossman, L. (1998). Accessibility of epitopes on UvrB protein in intermediates generated during incision of UV-irradiated DNA by the Escherichia coli Uvr(A)BC endonuclease. The Journal of biological chemistry *273*, 21009-21014.

Lammens, A., Schele, A., and Hopfner, K.P. (2004). Structural biochemistry of ATP-driven dimerization and DNA-stimulated activation of SMC ATPases. Curr Biol *14*, 1778-1782.

Laptenko, O., Kim, S.S., Lee, J., Starodubtseva, M., Cava, F., Berenguer, J., Kong, X.P., and Borukhov, S. (2006). pH-dependent conformational switch activates the inhibitor of transcription elongation. The EMBO journal *25*, 2131-2141.

Lindsley, J.E. (2001). Use of a real-time, coupled assay to measure the ATPase activity of DNA topoisomerase II. Methods in molecular biology (Clifton, NJ *95*, 57-64.

Ma, K., Temiakov, D., Anikin, M., and McAllister, W.T. (2005). Probing conformational changes in T7 RNA polymerase during initiation and termination by using engineered disulfide linkages. Proceedings of the National Academy of Sciences of the United States of America *102*, 17612-17617.

Moolenaar, G.F., Herron, M.F., Monaco, V., van der Marel, G.A., van Boom, J.H., Visse, R., and Goosen, N. (2000). The role of ATP binding and hydrolysis by UvrB during nucleotide excision repair. The Journal of biological chemistry *275*, 8044-8050.

Moolenaar, G.F., Hoglund, L., and Goosen, N. (2001). Clue to damage recognition by UvrB: residues in the beta-hairpin structure prevent binding to non-damaged DNA. The EMBO journal *20*, 6140-6149.

Moolenaar, G.F., Schut, M., and Goosen, N. (2005). Binding of the UvrB dimer to non-damaged and damaged DNA: residues Y92 and Y93 influence the stability of both subunits. DNA repair *4*, 699-713.

Myles, G.M., Hearst, J.E., and Sancar, A. (1991). Site-specific mutagenesis of conserved residues within Walker A and B sequences of Escherichia coli UvrA protein. Biochemistry *30*, 3824-3834.

Orelle, C., Gubellini, F., Durand, A., Marco, S., Levy, D., Gros, P., Di Pietro, A., and Jault, J.M. (2008). Conformational change induced by ATP binding in the multidrug ATP-binding cassette transporter BmrA. Biochemistry *47*, 2404-2412.

Orren, D.K., and Sancar, A. (1989). The (A)BC excinuclease of Escherichia coli has only the UvrB and UvrC subunits in the incision complex. Proceedings of the National Academy of Sciences of the United States of America *86*, 5237-5241.

Orren, D.K., and Sancar, A. (1990). Formation and enzymatic properties of the UvrB.DNA complex. The Journal of biological chemistry *265*, 15796-15803.

Pakotiprapha, D., Inuzuka, Y., Bowman, B.R., Moolenaar, G.F., Goosen, N., Jeruzalmi, D., and Verdine, G.L. (2008). Crystal Structure of Bacillus stearothermophilus UvrA Provides Insight into ATP-Modulated Dimerization, UvrB Interaction, and DNA Binding. Molecular cell *29*, 122-133.

Pakotiprapha, D., Samuels, M., Shen, K., Hu, J.H., and Jeruzalmi, D. (2012). Structure and mechanism of the UvrA-UvrB DNA damage sensor. Nature structural & molecular biology *19*, 291-298.

Panagiotidis, C.H., Reyes, M., Sievertsen, A., Boos, W., and Shuman, H.A. (1993). Characterization of the structural requirements for assembly and nucleotide binding of an ATP-binding cassette transporter. The maltose transport system of Escherichia coli. The Journal of biological chemistry *268*, 23685-23696.

Rossi, F., Khanduja, J.S., Bortoluzzi, A., Houghton, J., Sander, P., Guthlein, C., Davis, E.O., Springer, B., Bottger, E.C., Relini, A.*, et al.* (2011). The biological and structural characterization of Mycobacterium tuberculosis UvrA provides novel insights into its mechanism of action. Nucleic acids research *39*, 7316-7328.

Schneider, C.A., Rasband, W.S., and Eliceiri, K.W. (2012). NIH Image to ImageJ: 25 years of image analysis. Nat Methods *9*, 671-675.

Seeger, M.A., von Ballmoos, C., Eicher, T., Brandstatter, L., Verrey, F., Diederichs, K., and Pos, K.M. (2008). Engineered disulfide bonds support the functional rotation mechanism of multidrug efflux pump AcrB. Nature structural & molecular biology *15*, 199-205.

Seeley, T.W., and Grossman, L. (1990). The role of Escherichia coli UvrB in nucleotide excision repair. The Journal of biological chemistry *265*, 7158-7165.

Sharma, D., Say, A.F., Ledford, L.L., Hughes, A.J., Sehorn, H.A., Dwyer, D.S., and Sehorn, M.G. (2013). Role of the conserved lysine within the Walker A motif of human DMC1. DNA repair *12*, 53-62.

Sjoelund, V., and Kaltashov, I.A. (2007). Transporter-to-trap conversion: a disulfide bond formation in cellular retinoic acid binding protein I mutant triggered by retinoic acid binding irreversibly locks the ligand inside the protein. Biochemistry *46*, 13382-13390.

Skorvaga, M., Theis, K., Mandavilli, B.S., Kisker, C., and Van Houten, B. (2002). The beta - hairpin motif of UvrB is essential for DNA binding, damage processing, and UvrC-mediated incisions. The Journal of biological chemistry *277*, 1553-1559.

Thiagalingam, S., and Grossman, L. (1991). Both ATPase sites of Escherichia coli UvrA have functional roles in nucleotide excision repair. The Journal of biological chemistry *266*, 11395-11403.

Timmins, J., Gordon, E., Caria, S., Leonard, G., Acajjaoui, S., Kuo, M.S., Monchois, V., and McSweeney, S. (2009). Structural and mutational analyses of Deinococcus radiodurans UvrA2 provide insight into DNA binding and damage recognition by UvrAs. Structure *17*, 547-558.

Van Houten, B., Gamper, H., Sancar, A., and Hearst, J.E. (1987). DNase I footprint of ABC excinuclease. The Journal of biological chemistry *262*, 13180-13187.

Verhoeven, E.E., Wyman, C., Moolenaar, G.F., and Goosen, N. (2002). The presence of two UvrB subunits in the UvrAB complex ensures damage detection in both DNA strands. The EMBO journal *21*, 4196-4205.

Wagner, K., Moolenaar, G.F., and Goosen, N. (2010). Role of the two ATPase domains of Escherichia coli UvrA in binding non-bulky DNA lesions and interaction with UvrB. DNA repair *9*, 1176-1186.

Wagner, K., Moolenaar, G.F., and Goosen, N. (2011). Role of the insertion domain and the zinc-finger motif of Escherichia coli UvrA in damage recognition and ATP hydrolysis. DNA repair *10*, 483-496.

Webster, M.P., Jukes, R., Zamfir, V.S., Kay, C.W., Bagneris, C., and Barrett, T. (2012). Crystal structure of the UvrB dimer: insights into the nature and functioning of the UvrAB damage engagement and UvrB-DNA complexes. Nucleic acids research.

Zou, Y., Walker, R., Bassett, H., Geacintov, N.E., and Van Houten, B. (1997). Formation of DNA repair intermediates and incision by the ATP-dependent UvrB-UvrC endonuclease. The Journal of biological chemistry *272*, 4820-4827.